

Problem of Brownian Motion in a Periodic Potential

P. Fulde

Max-Planck-Institut für Festkörperforschung, Stuttgart, Germany

and

L. Pietronero, W. R. Schneider, and S. Strässler

Brown Boveri Research Center, CH-5401, Baden, Switzerland

(Received 10 September 1975)

We calculate the frequency-dependent mobility of a classical Brownian particle moving in a periodic potential. The problem is solved by applying a generalized version of Mori's continued-fraction method. The results are then used to interpret the observed frequency-dependent conductivity for the superionic conductor AgI.

In the classical theory of Brownian motion one investigates the motion of a particle in a given potential field under the influence of a stochastic force. The fluctuating force is responsible for energy dissipation of the moving particle via damping and the detailed form of this damping is connected with the spectrum of the random force by the fluctuation-dissipation theorem.¹ A particularly interesting model for Brownian motion is the case of a one-dimensional sinusoidal potential. The corresponding Langevin equation is

$$m\ddot{x} + m\gamma\dot{x} + m\omega_0^2 \frac{a}{2\pi} \sin \frac{2\pi}{a}x = f(t), \quad (1)$$

where m is the mass of the particle, γ is the damping, and $\omega_0^2 = (2\pi)^2 A/2ma^2$, with A the barrier height and a the lattice constant. We assume that the stochastic force $f(t)$ has a white power spectrum,¹ i.e., $\langle f(t)f(0) \rangle_T = 2m\gamma K_B T \delta(t)$, where $\langle \dots \rangle_T$ denotes a thermal average and K_B and T are the Boltzmann constant and temperature, respectively. Equation (1) can be viewed as describing a pendulum under the influence of a random force if x denotes the angular deviation from the equilibrium position. It also describes fluctuations of the Josephson supercurrent through a tunneling junction.^{2,3} In that case $(2\pi/a)x$ denotes the phase of the superconducting order parameter and m , $(m\gamma)^{-1}$, and $m\omega_0^2$ are the capacitance, the resistance, and the coupling energy of the tunnel contact. Equation (1) is also the simplest model for describing the diffusion of an impurity atom in a crystal⁴ and, more generally, superionic conductance.⁵ In that case the $x_n = a(\frac{3}{4} + n)$ (n being an integer) denote the different equilibrium sites for the ions. It is particularly the model description of superionic conductors by Eq. (1) which has stimulated the present in-

vestigation and we will refer to this as well as to possible extensions. Finally we point out that Eq. (1) also occurs in the problems of Bloch-wall motion, propagation in nerve fibers, Fröhlich superconductors, etc.

Our aim will be to derive from Eq. (1) an expression for the velocity-velocity correlation function $\langle \dot{x}(t)\dot{x}(0) \rangle_T$. It will enable us to compute the frequency-dependent mobility $\mu(\omega)$ via

$$\mu(\omega) = (K_B T)^{-1} \int_0^\infty dt e^{i\omega t} \langle \dot{x}(t)\dot{x}(0) \rangle_T. \quad (2)$$

This mobility will contain oscillatory as well as diffusive features. It is therefore expected to be able to reproduce the physics of superionic conductors. The comparison with other model calculations can be readily made.^{5,6}

There exist some analytic results for $\mu(\omega=0, T)$ in certain limiting cases. In the low-temperature limit ($K_B T \ll A$) one obtains⁷

$$\mu(0, T) = (a^2/2\pi K_B T) [(\frac{1}{4}\gamma^2 + \omega_0^2)^{1/2} - \frac{1}{2}\gamma] e^{-2v}, \quad (3)$$

where $v = A/2K_B T = m\omega_0^2 a^2/4\pi^2 K_B T$. Furthermore in the limit of vanishing damping ($\gamma \rightarrow 0$) one finds⁸

$$\mu(0, T) = \frac{1}{2} a (2\pi m K_B T)^{-1/2} \frac{I_0(v) + I_1(v)}{I_0^2(v)} e^{-v}, \quad (4)$$

where $I_\nu(v)$ denote Bessel functions. Finally, in the limit of large damping (zero capacitance in the Josephson-noise problem), we have²

$$\mu(0, T) = (m\gamma)^{-1} [I_0^2(v)]^{-1}. \quad (5)$$

The physical region of the parameters for superionic conductors ($A \sim 0.1$ eV, $m \sim 100m_{\text{proton}}$, $\omega_0 \sim 100$ cm⁻¹, $\gamma \sim 50$ cm⁻¹) can be generally described simply by Eq. (4). Furthermore, by interpolating between the different cases one can obtain good approximations for $\mu(0)$ for any val-

ue of γ and ν .

In order to compute $\mu(\omega, T)$ we use a generalization for non-Hamiltonian systems⁹ of the method employed by Mori for Hamiltonian systems.^{10,11} The continued fraction can be now written in the form¹²

$$\mu(\omega) = \frac{1}{m} \frac{1}{-i\omega - \gamma_0 + \frac{\Delta_1}{-i\omega - \gamma_1 + \dots + \frac{\Delta_{n-1}}{-i\omega + G_n(\omega, T)}}} \quad (6)$$

For the case of sinusoidal potential given by Eq. (1) the terms γ_k and Δ_k ($k=1, \dots, n$) up to $n=4$ are $\gamma_0 = -\gamma$, $\gamma_1 = 0$, $\gamma_2 = -\gamma$ and $\Delta_1 = \omega_0^2 \alpha$, $\Delta_2 = \omega_0^2 \times \beta$, $\Delta_3 = \omega_0^2 (4\beta^{-1} \nu^{-2} - \alpha^{-1})$, with $\alpha = I_1(\nu)/I_0(\nu)$ and $\beta = \alpha^{-1} - \nu^{-1} - \alpha$. It is interesting to compare the continued fraction (6) with the mobility of a damped harmonic oscillator of frequency ω_0 :

$$\mu(\omega) = \frac{1}{m - i\omega + \gamma + \omega_0^2 / (-i\omega)} \quad (7)$$

The expression (7) can be obviously obtained from Eq. (6) in the limit of low temperature. At finite temperatures, because of anharmonicity, the frequency ω_0 is replaced by an effective frequency $\bar{\omega}_0^2 = \omega_0^2 I_1(\nu)/I_0(\nu)$. Furthermore other terms are added to Eq. (7) in the continued-fraction form (6) that can give rise to diffusion [$\mu(\omega=0) \neq 0$]. The exact form of $G_n(\omega, T)$ in Eq. (6) is not needed here as we approximate it by $g_n(T)$ in such a way that the static mobility $\mu(0, T)$ is reproduced correctly, i.e., in accordance with the expressions given above. It turns out that with $g_n(T)$ fixed in that way the convergence of the continued-fraction method is good. Some numerical results for $\text{Re}\mu(\omega)$ calculated up to $n=4$ are shown in Fig. 1. They correspond to the parameters $A=0.1$ eV, $\nu=1.28$, $a=5$ Å, and $\gamma=50$ cm⁻¹. The numbers associated to each line in Fig. 1 correspond to the point where the continued fraction was stopped. $\mu(0)$ was derived using Eq. (4) which is appropriate for the considered parameters.

Let us note, at this point, that a more phenomenological approach can be used to describe a diffusing oscillator by introducing the memory-function approximation.⁵ Instead of Eq. (1) we have the following equation of motion:

$$m\ddot{x} + m\gamma\dot{x} + m\bar{\omega}_0^2 \int_{t_0}^t M(t-t')\dot{x}(t') dt' = f(t), \quad (8)$$

$\bar{\omega}_0$ being an effective frequency and M the memory function given by

$$M(t-t') = \exp[-(t-t')/\tau], \quad (9)$$

where τ is the critical time between oscillatory and diffusive behavior. This method provides an expression for the frequency-dependent mobility equal to the continued fraction with $n=2$. Therefore the continued-fraction method justifies the phenomenological memory-function approach because the case $n=2$ already gives a good approximation to the more accurate results obtained by including higher terms in the continued-fraction method (see Fig. 1).

Let us now extend the problem to include the possibility that the Brownian particle interacts with its surroundings. In the simplest case the particle creates a local lattice deformation which follows the hopping motion. This resembles closely the polaron picture. In a more realistic case one should also include the interaction with other Brownian particles, but this goes beyond the simple single-particle picture we wish to

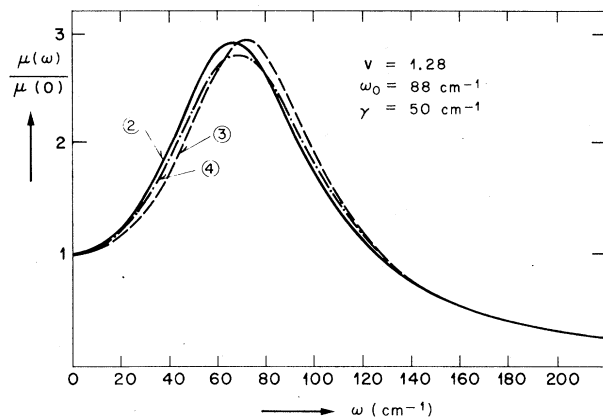


FIG. 1. Numerical evaluation of $\text{Re}\mu(\omega)$ as given by Eq. (6) up to $n=4$. The value of $\mu(0)$ is derived using Eq. (4). The curve with $n=2$ practically corresponds to the phenomenological memory-function approach (Ref. 5) [Eq. (8)] that can be considered a reliable approximation because of the good convergence obtained using the continued-fraction approach. The case $n=1$, not shown in the figure, corresponds simply to a Drude behavior.

present here. If X denotes the center of the lattice deformation, we replace Eq. (1) by

$$m\ddot{x} + m\gamma\dot{x} + m\omega_0^2 \frac{a}{2\pi} \sin \frac{2\pi}{a} x + m\Omega_0^2(x - X) = f(t), \quad (10)$$

where Ω_0 is a measure of the restoring force due to the interaction with the surroundings. For X we assume the following equation to hold:

$$M\ddot{X} + M\Gamma\dot{X} - M\Omega_0^2(x - X) = F(t). \quad (11)$$

Here Γ and $F(t)$ are the damping and the stochastic force. Equations (10) and (11) could be solved by the continued-fraction method extended to many variables.¹² Here we consider instead the simple phenomenological memory-function approach [see Eq. (8)] which in view of our findings for Eq. (1) seems to us fully justified. The expression for the frequency-dependent mobility becomes now

$$\mu(\omega) = \frac{-i\omega BK_B T/m}{AB - (m/M)\Omega_0^4}, \quad (12)$$

where

$$A = \Omega_0^2 - \omega^2 - i\omega\gamma - i\omega\bar{\omega}_0^2 \hat{M}(\omega), \quad (13)$$

$$\hat{M}(\omega) = (-i\omega + 1/\tau)^{-1},$$

$$B = (m/M)\Omega_0^2 - \omega^2 - i\omega\Gamma. \quad (14)$$

In Fig. 2 $\sigma_{\text{expt}}(\omega)$ has been determined by a Kramers-Kronig (KK) analysis of the observed reflectivity of AgI at $T = 453^\circ\text{K}$. At frequencies above $\sim 20 \text{ cm}^{-1}$, $\sigma(\omega)$ is qualitatively the same as predicted by the model corresponding to Eq. (1). The dotted part of $\sigma(\omega)$ below 10 cm^{-1} depends strongly on the extrapolation procedures used in the KK analysis but agrees with transmission measurements by Funke and Jost.¹³ Their results show further structure in $\sigma(\omega)$ at microwave frequencies ($\sim 1 \text{ cm}^{-1}$). The dashed curve in Fig. (2) corresponds to Eq. (12) using the following parameters (in cm^{-1}): $\bar{\omega}_0 = 104$, $\Omega_0 = 15$, $\gamma = 45$, $1/\tau = 53$, and $(M/m)\Gamma = 260$. Note that the simple polaron theory as represented by Eq. (12) can in principle explain the decrease in $\sigma(\omega)$ at $\omega \sim 20 \text{ cm}^{-1}$ but it gives no further fine structure below that value. To describe this structure one then probably has to consider the detailed many-body interactions.

In conclusion we have shown that a single-particle model that properly includes both oscillatory and diffusive behavior [Eq. (1)] can be treat-

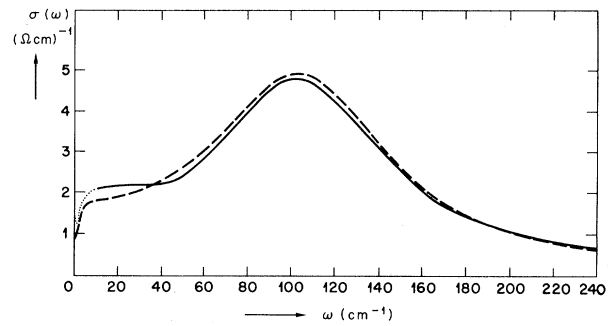


FIG. 2. $\sigma(\omega)$ for the superionic conductor AgI as measured by Brüesch, Strässler, and Zeller (Ref. 5) (solid line). The dashed line represents the theoretical results from Eq. (12). For the parameters used see the text. The prefactor to go from $\mu(\omega)$ to $\sigma(\omega)$ is the same as in Ref. 5.

ed by means of the simple memory-function method. This model can describe most of the features of the frequency-dependent mobility of a superionic conductor (AgI). We remark that this approach is basically different from the one recently employed by Huberman and Sen⁶ in which the mobility is directly written as the sum of a diffusion term and a distribution of oscillators. Some of the features of the low-frequency region ($\omega \lesssim 20 \text{ cm}^{-1}$) can then be understood in terms of interaction with the lattice. The next step would be the extension of Eqs. (10) and (11) to include the correlation between diffusing particles. This work was initiated by many discussions with Dr. P. Brüesch and Dr. H. R. Zeller. Especially Dr. Zeller has contributed to the interpretation of the experimental conductivity. We also would like to thank Dr. Brüesch for making his experimental results available to us before publication.

¹R. Kubo, Rep. Prog. Phys. **29**, 225 (1966).

²Y. M. Ivanchenko and L. A. Zil'berman, Zh. Eksp. Teor. Fiz. **55**, 2395 (1968) [Sov. Phys. JETP **28**, 1272 (1969)].

³V. Ambegaokar and B. I. Halperin, Phys. Rev. Lett. **22**, 1364 (1969); M. J. Stephen, Phys. Rev. **186**, 393 (1969); D. Rogovin and D. J. Scalapino, Ann. Phys. (New York) **86**, 1 (1974).

⁴J. H. Weiner and R. E. Froman, Phys. Rev. B **10**, 315 (1974).

⁵P. Brüesch, S. Strässler, and H. R. Zeller, Phys. Status Solidi (a) **31**, 217 (1975).

⁶B. A. Huberman and P. N. Sen, Phys. Rev. Lett. **33**, 1379 (1974).

⁷S. Chandrasekhar, Rev. Mod. Phys. **15**, 68 (1943).

⁸C. A. Wert, Phys. Rev. **79**, 601 (1950).

⁹The terms of the continued fraction are now derived

from the Fokker-Planck operator corresponding to the Langevin equation (1) (see W. R. Schneider, to be published).

¹⁰H. Mori, Prog. Theor. Phys. Jpn. 33, 423 (1965).

¹¹R. Kubo, in *Many Body Theory: Tokyo Summer In-*

stitute Lectures in Theoretical Physics, 1965, edited by R. Kubo (Benjamin, New York, 1966), Pt. 1.

¹²Schneider, Ref. 9.

¹³K. Funke and A. Jost, Ber. Bunsenges. Phys. Chem. 75, 436 (1971).

4f-Virtual-Bound-State Formation in CeAl₃ at Low Temperatures

K. Andres and J. E. Graebner

Bell Laboratories, Murray Hill, New Jersey 07974

and

H. R. Ott

Laboratorium für Festkörperphysik, Eidgenössische Technische Hochschule, Hönggerberg, Zürich, Switzerland

(Received 25 August 1975)

Specific-heat and electrical-resistivity measurements in CeAl₃ below 0.2 K reveal enormous magnitudes of the linear specific-heat term $C = \gamma T$ ($\gamma = 1620$ mJ mole/K²) and the T^2 term in $\rho = AT^2$ ($A = 35 \mu\Omega$ cm/K²). We conclude that the 4f electrons obey Fermi statistics at low temperatures because of the formation of virtual bound 4f states.

In the intermetallic compound CeAl₃ both the lattice parameters and the susceptibility at high temperatures suggest that the Ce ion is in a 3+ state. The lack of magnetic order at low temperatures is interpreted as being caused by a partial admixture of the nonmagnetic 4+ state. Such behavior has been explained in different ways in the past. A model distinguishing between "atomic" and "bandlike" 4f electrons has been suggested by Gschneidner.¹ More recently, CeAl₃ has often been cited as an example of a mixed valence—or interconfigurational fluctuation (ICF)—compound²; and in another approach, Mott³ has explained the peculiar properties of CeAl₃ based on a Kondo-type theory. The purpose of this note is to present new data on the very-low-temperature properties of CeAl₃ and to show that they can be understood using Friedel's⁴ classic theory of virtual bound states.

All measurements were performed in dilution refrigerators except the thermal-expansion measurement, which was done in a ³He cryostat. The data were taken by standard techniques using a cerium-magnesium-nitrate magnetic-susceptibility thermometer. Only polycrystalline samples were investigated; they were cut from a 20-g button that was arc melted in argon and annealed at 900°C for 3 weeks. X-ray analysis showed the proper structure (hexagonal, Ni₃Sn-type). The specific-heat results are shown in Fig. 1. Below 150 mK, the specific heat varies

linearly with temperature and yields an extremely large γ value of 1620 mJ/mole K². It remains practically unchanged in a field of 10 kOe except at the lowest temperatures where the nuclear Zeeman specific heat of the Al nuclei is seen (the Ce¹⁴⁰ and Ce¹⁴² isotopes have no nuclear spin). This behavior is to be contrasted with what one would have expected from the lowest-lying Ce³⁺ Kramers doublet state, namely a strong field-dependent magnetic specific heat with entropy $R \ln 2$ /mole. Interpolating our data with previous specific-heat measurements down

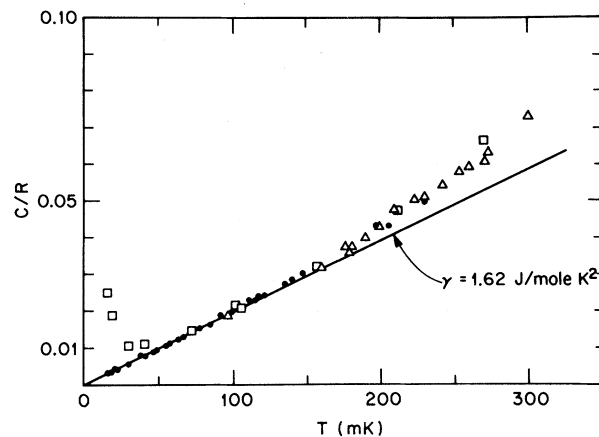


FIG. 1. Specific heat of CeAl₃ at very low temperatures in zero field (●, Δ) and in 10 kOe (□).